



Article

Impacts of Climate Change and Human Activity on Lakes around the Depression of Great Lakes in Mongolia

Song Yang ^{1,2}, Hongfei Zhou ^{1,*}, Yan Liu ¹, Batsuren Dorjsuren ³ , Otgonbayar Demberel ⁴  and Dashlkham Batmunkh ³

¹ Xinjiang Institute of Ecology and Geography, Chinese Academy of Sciences, Urumqi 830011, China; yangsong21@mailsucas.ac.cn (S.Y.); liuyan@ms.xjb.ac.cn (Y.L.)

² University of Chinese Academy of Sciences, Beijing 100049, China

³ School of Engineering and Applied Sciences, National University of Mongolia, Ulaanbaatar 210646, Mongolia; batsuren@seas.num.edu.mn (B.D.); dashlkhamb@mailsucas.ac.cn (D.B.)

⁴ Khovd Branch School, National University of Mongolia, Khovd 164300, Mongolia; otgonbayar.d@num.edu.mn

* Correspondence: zhouhf@ms.xjb.ac.cn

Abstract: The western region of Mongolia is characterized by an arid climate and a fragile ecological environment. It is a sensitive zone in response to global climate change and one of the major sources of dust globally. This region is home to numerous lakes, and their dynamic changes not only reflect global climate variations but also have implications for the global ecological environment quality. In this study, Landsat images were used as the data source, and Google Earth Engine (GEE) was employed to extract lakes with an area larger than 1 km² from 1992 to 2021. The spatiotemporal characteristics of lake water area (LWA) changes were analyzed, and a structural equation model was applied to attribute the lake changes. The results indicate an overall trend of increasing lake area followed by a decrease in the study area. Specifically, lakes in the provinces of Khovd and Gobi-Altai exhibited a decreasing trend followed by an increasing trend, while lakes in the provinces of Uvs and Zavkhan showed an increasing trend followed by a decreasing trend. Three typical types of lakes, namely, alpine lakes, throughflow lakes, and terminal lakes, all exhibited a trend of increasing area followed by a decrease. The analysis of driving forces behind lake area changes reveals that climate change and human activities primarily exert indirect influences on the lake area changes in each province. Specifically, climate change and human activities lead to changes in soil moisture, which have a significant explanatory power for lake area changes. Regarding the typical types of lakes, climate change serves as the primary driving force for alpine lakes, while human activities are the main driving forces for throughflow lakes and terminal lakes.

Keywords: western Mongolia; lakes; arid regions; temporal and spatial changes; influencing factors; remote sensing



Citation: Yang, S.; Zhou, H.; Liu, Y.; Dorjsuren, B.; Demberel, O.; Batmunkh, D. Impacts of Climate Change and Human Activity on Lakes around the Depression of Great Lakes in Mongolia. *Land* **2024**, *13*, 310. <https://doi.org/10.3390/land13030310>

Academic Editor: Adrianos Retalis

Received: 2 January 2024

Revised: 30 January 2024

Accepted: 8 February 2024

Published: 29 February 2024



Copyright: © 2024 by the authors. Licensee MDPI, Basel, Switzerland. This article is an open access article distributed under the terms and conditions of the Creative Commons Attribution (CC BY) license (<https://creativecommons.org/licenses/by/4.0/>).

1. Introduction

Lakes in arid regions are highly sensitive to climate change and human activities; they are often regarded as sensitive indicators of climate and environmental changes in arid areas [1]. However, in recent years, due to global changes and intensified human activities [2], lakes in arid regions are facing severe shrinkage issues [3]. The loss of water resources in lakes has also triggered a series of ecological issues, including wetland area reduction, water salinization, deterioration of water quality, and decline in biodiversity, severely compromising the ecosystem services value of lakes in arid regions. This has constrained the sustainable development of the local economy and society [3].

The western region of Mongolia, with the Great Lakes Depression at its core, exemplifies a typical arid area that has undergone notable lake transformations in recent decades [4,5]. The changes observed in the lakes surrounding the Great Lakes Depression

serve as a representative example for the entire Mongolian Plateau and the arid zone of Central Asia. Firstly, occupying a significant physiographic position in Central Asia, western Mongolia stands out as a distinctive region characterized by towering mountains, contemporary glaciers, expansive tectonic depressions, intermontane valleys, as well as vast rivers and lakes [6]. Lake areas in this region account for 59.7% of the country's total lake area [6], rendering them a crucial water source for both agricultural production and the livelihoods of inhabitants within the arid and cold environment of the region [7]. Secondly, the Great Lakes Depression in Mongolia assumes a pivotal climatic role, serving as a crucial link between the Pacific and Atlantic-influenced climates [8]. It stands as a climatically sensitive area that has witnessed significant warming in recent years [9]. Climate change, escalating human activities, and the melting of glaciers are recognized as the primary factors influencing lake dynamics in Central Asia [10–12], with all three factors occurring simultaneously and exerting a substantial impact in and around the Great Lakes Depression [6,13]. Specifically, western Mongolia occupies an intermediate zone between the Siberian taiga forest in the north and the Gobi desert in the south, residing within a region characterized by the highest level of continentality across Eurasia [6,13]. This unique setting is developed under the interplay of three large-scale climatic systems: the Siberian high-pressure cell, the Asian low-pressure cell, and the westerlies. Owing to its exceptional physiographic conditions, extensive proliferation of numerous lakes, and its pristine, untamed, and less anthropogenically impacted nature, the lakes in western Mongolia serve as a natural repository, resembling a museum of the northeastern and eastern Eurasian continent [6,13].

According to research, in recent years, overgrazing and intensified human activities in Mongolia have led to a rapid and sudden increase in land degradation in certain areas [14,15]. Climate factors and land degradation have formed a positive feedback loop between insufficient soil moisture and surface warming in the region, leading to a hotter and drier climate [15,16]. Unprecedented droughts have occurred in the country in recent years, which inevitably have significant impacts on the numerous lakes distributed in western Mongolia [4,5,7,17,18]. However, the current selection of driving factors for lake changes has mainly focused on meteorological and socio-economic factors, with less emphasis on soil environment [5,7]. Furthermore, there is a lack of research on the mechanisms by which these influencing factors affect lake changes. In light of these circumstances, this study utilizes Landsat remote sensing images as data sources to extract lakes larger than 1 square kilometer in western Mongolia from 1992 to 2021 and analyzes their spatial and temporal changes. By combining meteorological, socio-economic, and soil moisture data, a structural equation model is employed to quantify the impacts of climate change and human activities on lake changes.

2. Study Area

As shown in Figure 1, the western five provinces to the west of Mount Hangai in Mongolia were selected as the study area, including Khovd province (76,012.72 km²), Bayan-Ulgii province (45,748.99 km²), Gobi-Altai province (141,855.24 km²), Uvs province (69,595.47 km²), and Zavkhan province (82,620.94 km²), with a total area of 415,833.37 km². The western part of Mongolia exhibits diverse landforms with significant topographical variations, ranging in elevation from 524 to 4323 m above sea level, with an average elevation of 1822 m. The region is characterized by a rich landscape, including high mountains, modern glaciers, large structural basins, mountain valleys, as well as major rivers and lakes. The western region of Mongolia is an important climatic zone, situated under the influence of three major atmospheric circulations: the Siberian anticyclone, the westerlies, and the Central Asian cyclone. It is also affected by air masses from the Atlantic Ocean and the Arctic Ocean. However, the air masses from these two oceans are blocked by the Altai Mountains and cannot penetrate into Mongolia [6]. This phenomenon results in widespread aridity throughout the entire region. The annual average precipitation in the five major basin areas is between 100 and 150 mm, while in the Mongolian Altai Mountains,

the annual average precipitation ranges from 150 to 300 mm. According to records from the Ulgii and Khovd meteorological stations, the average annual temperature in the area is 1.8 °C. The summer monthly average temperature in Khovd reaches as high as 19 °C, while in winter, the monthly average temperature drops to −25.5 °C, indicating a typical continental climate characteristic [6].

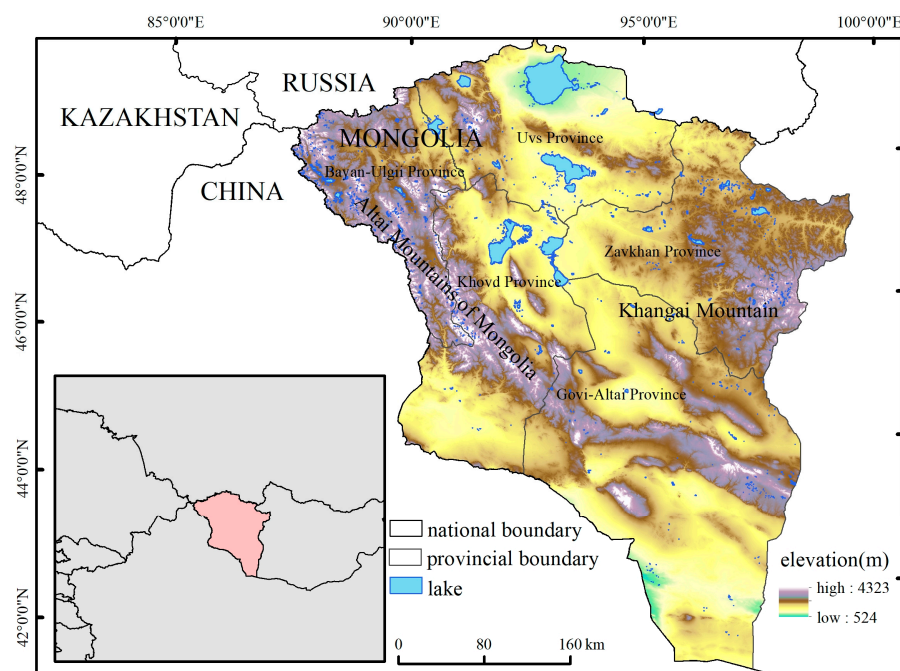


Figure 1. The western range and topography of Mongolia. Note that this map is based on the standard map (No. GS (2019) 1822) of the Map Service System (<http://bzdt.ch.mnr.gov.cn/>) marked by the Ministry of Natural Resources of the People’s Republic of China, and the base map has not been modified.

3. Data and Methods

3.1. Data Sources

Utilizing the Google Earth Engine (GEE) platform, we acquired remote sensing images (Landsat 5 TM, Landsat 7 ETM+, and Landsat 8 OLI) with a spatial resolution of 30 m from 1992 to 2021 in the western region of Mongolia to extract water body information. A total of 18,554 satellite images were used in this study, including approximately 6543 images from Landsat 5, approximately 8132 images from Landsat 7, and approximately 3869 images from Landsat 8 (Figures S1 and S2). All these images were derived from the Google Earth Engine (GEE) (<https://earthengine.google.org/>).

Changes in the lake area are influenced by climate change, human activities, and the soil environment. Meteorological data was obtained from CHELSA (Climatologies at high resolution for the earth’s land surface areas) (<http://chelsa-climate.org/>), which is a very high resolution (the temporal resolution is monthly, and the spatial resolution is 1 km) global downscaled climate data set currently hosted by the Swiss Federal Institute for Forest. This study selected the annual precipitation (AP), summer mean temperature (SMT), and potential evapotranspiration (PET) data from the CHELSA dataset for the period from 1992 to 2018. To evaluate the intensity of human activities, we utilized data from the National Statistical Office of Mongolia (<http://1212.mn/mn>) for the years 1992 to 2018, including indicators such as irrigation, grazing, and population. The soil moisture data from 1992 to 2018 is derived from ERA5-Land, with a monthly temporal resolution and a spatial resolution of $0.1^\circ \times 0.1^\circ$. ERA5-Land is the latest land component dataset within the fifth-generation reanalysis product from the European Centre for Medium-Range Weather Forecasts (ECMWF). ERA5-Land divides the soil profile into four layers: 0–7 cm, 7–28 cm,

28–100 cm, and 100–289 cm. In this study, the four soil moisture layers are represented as follows: the first layer of soil moisture (0–7 cm) is denoted as SM1, the second layer (7–28 cm) as SM2, the third layer (28–100 cm) as SM3, and the fourth layer (100–289 cm) as SM4. The meteorological data and soil moisture data were both clipped and merged using ArcGIS 10.8.2. Trend analysis of the meteorological data and soil moisture data was conducted using the Mann–Kendall test and Sen’s slope estimator on the Matlab platform.

3.2. Water Extraction and Processing

(1) Data preprocessing

To begin with, the CFMASK algorithm is employed within the GEE platform to effectively eliminate clouds and snow from the images [7,19], which works well and is suitable for preparing Landsat data for change detection. Furthermore, Digital Elevation Models (DEMs) are utilized to mask terrain shadows, resulting in a high-quality image set that is devoid of clouds, snow, and terrain shadows. Next, for each of the Landsat 5/7/8 data sources, the GEE platform is used to process the individual scene images by removing cloud and snow cover and then stacking them along the time axis (seasons) to create an image dataset containing only clear-sky observations [7,11,12]. Finally, the three sets of valid remote sensing image datasets are stacked throughout the year to create the final time series Landsat dataset of valid observations, which is used for extracting lake information. [7]. Since different remote sensing image data sources may use the same band names but correspond to different frequencies, it is necessary to rename the bands before image synthesis to ensure accuracy.

(2) Water body identification rules

The relationship between water bodies and vegetation indices has been widely utilized in surface water monitoring [20]. In this study, we employ a combination of three indices, namely, the Modified Normalized Water Body Index (MNDWI), the Normalized Vegetation Index (NDVI), and the Enhanced Vegetation Index (EVI), to identify water bodies. Previous research has demonstrated that $MNDWI > NDVI$ or $MNDWI > EVI$ serves as a reliable criterion for distinguishing between water and non-water bodies [7,12,21]. Additionally, an EVI value below 0.1 ensures the removal of vegetated pixels or pixels that contain a mixture of water and vegetation [7,12]. Therefore, in our study, we identify water bodies based on the criteria of $MNDWI > NDVI$ or $MNDWI > EVI$ and $EVI < 0.1$. This approach offers greater stability compared to relying solely on individual indices for identification [7,12]. The formula used is as follows:

$$MNDWI = \frac{(\rho_{Green} - \rho_{Swir1})}{(\rho_{Green} + \rho_{Swir1})}, \quad (1)$$

$$NDVI = \frac{(\rho_{Nir} - \rho_{Red})}{(\rho_{Nir} + \rho_{Red})}, \quad (2)$$

$$EVI = 2.5 \times \frac{\rho_{Nir} - \rho_{Red}}{\rho_{Nir} + 6 \times \rho_{Red} - 7.5 \times \rho_{Blue} + 1}, \quad (3)$$

where ρ_{Blue} , ρ_{Green} , ρ_{Red} , ρ_{Nir} , and ρ_{Swir1} are the surface reflectance values of the blue (0.45–0.52 μm), green (0.52–0.60 μm), red (0.63–0.69 μm), near-infrared (NIR) (0.77–0.90 μm), and shortwaveinfrared-1 (SWIR1) (1.55–1.75 μm) bands in the Landsat TM, ETM+, and OLI sensors.

For each Landsat image element in the study area, the following equation calculates its water body frequency over the course of a year:

$$F(y) = \frac{1}{N_y} \sum_{i=1}^{N_y} w_{y,i} \times 100\%, \quad (4)$$

where F is the water frequency of the pixel, y is the specified year, N_y is the number of total Landsat observations of the pixel in that year, $w_{y,i}$ denotes whether one observation of the pixel is water, with one indicating water and zero indicating non-water. The water body

area was obtained from the water body frequency map by setting the threshold value, and the permanent water body area was obtained by setting the water body frequency to 0.75 based on the experience of previous studies [7].

(3) Accuracy verification

In this study, we employed a random sampling method, with a split of 75% for the training set and 25% for the validation set, to assess the accuracy of water body identification based on high-resolution images obtained from the GEE platform. We selected four distinct time periods for surface water data analysis: 1992, 2000, 2010, and 2020. Through visual interpretation, we uniformly chose 500 water points and 500 non-water points, resulting in a total of 1000 sample points. The validation outcomes demonstrated high accuracy in the spatial distribution of water bodies for each time period. Specifically, the overall accuracy (measured by the Kappa coefficient) for 1992, 2000, 2010, and 2020 were found to be 97.4% (0.93), 96.8% (0.92), 96.2% (0.90), and 95.8% (0.89), respectively. The mean overall accuracy and Kappa coefficient across all time periods were calculated as 96.55% and 0.91, respectively. These results indicate that the extracted water body information exhibits a high level of accuracy, meeting the requirements for subsequent studies. By employing the random sampling method and carefully interpreting the high-resolution images, we have obtained reliable validation results, affirming the accuracy and suitability of the water body extraction for further research purposes.

3.3. Methods for Attributing Inter-Annual Trends in Lake Area

Structural equation modeling (SEM) enables researchers to conduct a comprehensive analysis of causal relationships between multiple variables within complex systems. It facilitates the exploration of both direct and indirect relationships between variables, shedding light on the intricate interconnections within the system. Additionally, SEM facilitates the examination of latent variables, which are artificial constructs that cannot be directly measured but play a crucial role in influencing the observed variables. By incorporating SEM into our research methodology, we can gain a deeper understanding of the complex dynamics and interdependencies within the studied system.

In contrast to traditional SEM, the most evident characteristic of PLS-SEM (Partial least squares structural equation model) is that it does not strictly follow the standardized normal distribution assumptions for the observed variables [22]. There are two sub-models (measurement and structural) involved in PLS-SEM. The measurement model connects the observed variables (also called manifest variables) with their corresponding latent variables and is also called an external model. The structural model connects the latent variables with arrows from exogenous to endogenous latent variables, calculates the effects of the influence between the routes and is also called an internal model.

In the structural model, the linear relationship between the endogenous latent variable ζ_j and exogenous latent variable ζ_i can be written as:

$$\zeta_j = \sum_{i \neq j} \beta_{ji} \zeta_i + \zeta_j \quad (5)$$

where β_{ji} is the route coefficient between the latent variables. ζ_j is a random error.

In the measurement model, each latent variable is described by a linear combination of the observed variable (x_{jh}):

$$x_{jh} = \lambda_{jh} \zeta_j + \varepsilon_{jh} \quad (6)$$

where λ_{jh} is the coefficient of the column vector (ζ_j), and ε_{jh} is the random error. PLS modeling standardizes each latent variable to obtain a unit variance ($\text{Var}(\zeta_j) = 1$), to achieve scales for unambiguity.

4. Results and Discussion

4.1. Changes in Lakes $> 1 \text{ km}^2$ in the Great Lakes Depression and Adjacent Areas from 1992 to 2021

Information was extracted on lakes larger than 1 km^2 for each year from 1992 to 2021, and inter-annual trends in the lake area and number were analyzed. To better describe the changes in different-sized lakes, the lakes were categorized into three classes [5,7]: small ($1\text{--}10 \text{ km}^2$), medium ($10\text{--}50 \text{ km}^2$), and large lakes ($>50 \text{ km}^2$). It was found that there was a large inter-annual variation in the area and number of lakes in western Mongolia; the lake area shows an increasing trend from 1992 to 1996 and a decreasing trend from 1996 to 2021 (Figure 2).

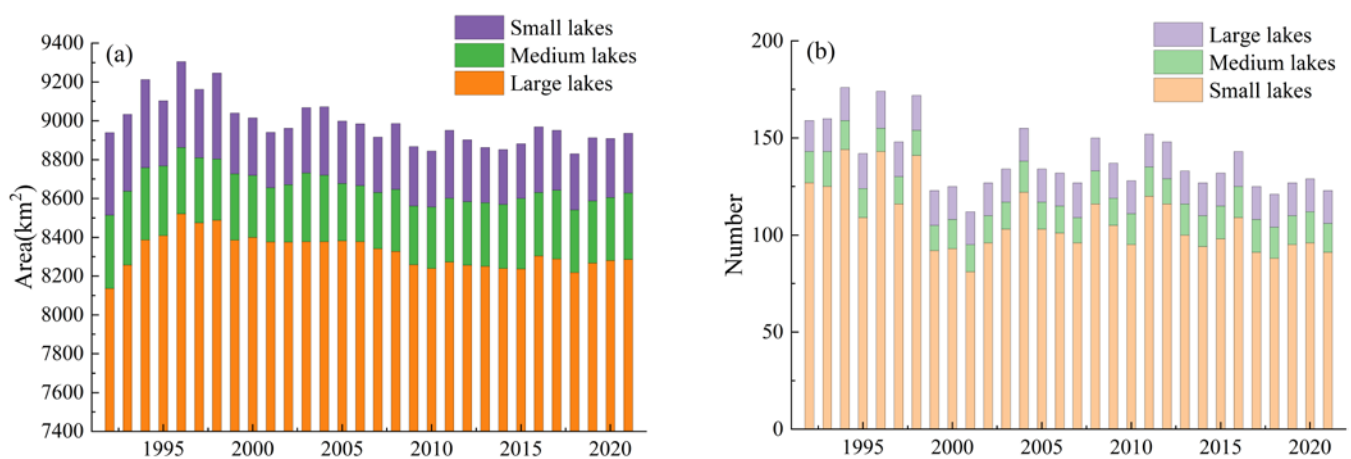


Figure 2. Interannual changes of lake area (a) and number (b) in western Mongolia from 1992 to 2021.

The total area of lakes increased from 8939.18 km^2 in 1992 to 9304.32 km^2 in 1996, an increase of 365.1 km^2 , with a rate of change of 4.08% , of which the area of small lakes increased by 17.01 km^2 , the area of medium lakes decreased by 36.04 km^2 , and the area of large lakes increased by 384.17 km^2 (Figure 2). The total area of lakes decreased from 9304.32 km^2 in 1996 to 8935.93 km^2 in 2021, with a decrease of 368.39 km^2 , and the rate of change was 3.96% , of which the area of small lakes decreased by 134.54 km^2 , the area of medium-sized lakes decreased by 1.03 km^2 and the area of large lakes decreased by 368.39 km^2 . The small, medium, and large lakes contributed 36.52% , 0.27% , and 64.57% , respectively, to the lake area decrease. The total number of lakes increased from 159 in 1992 to 174 in 1996, which is an increase of 15, with an increase of 15 small lakes, a decrease of 1 medium lake, and an increase of 1 large lake. The total number of lakes decreased from 174 to 123 between 1996 and 2021, which is a decrease of 51 lakes, all of which were small lakes.

4.2. Lake Changes in Different Administrative Regions of Western Mongolia

In order to analyze the spatial differentiation characteristics of lake area changes in western Mongolia, we analyzed lake dynamics for each administrative region in western Mongolia (Figure 3). In Khovd and Gobi-Altai provinces, the lake area decreased at a rate of 13.72 km^2 and 4.15 km^2 per year, respectively, from 1992 to 2001; in Gobi-Altai province, the lake area increased at a rate of 2.74 km^2 per year from 2001 to 2021, while in Khovd province it fluctuated considerably after 2001. The overall trend of lake area in Bayan-Ulgii province is decreased and concentrated from 1998 to 2001 ($-40.97 \text{ km}^2/\text{year}$, $R^2 = 0.96$), with a more moderate change in lake area after 2001. For Uvs and Zavkhan provinces, the lake area increased at the rate of 62.35 km^2 and 9.34 km^2 per year between 1992 and 1996, respectively, and decreased at the rate of 9.14 km^2 and 2.58 km^2 per year between 1996 and 2021, respectively.

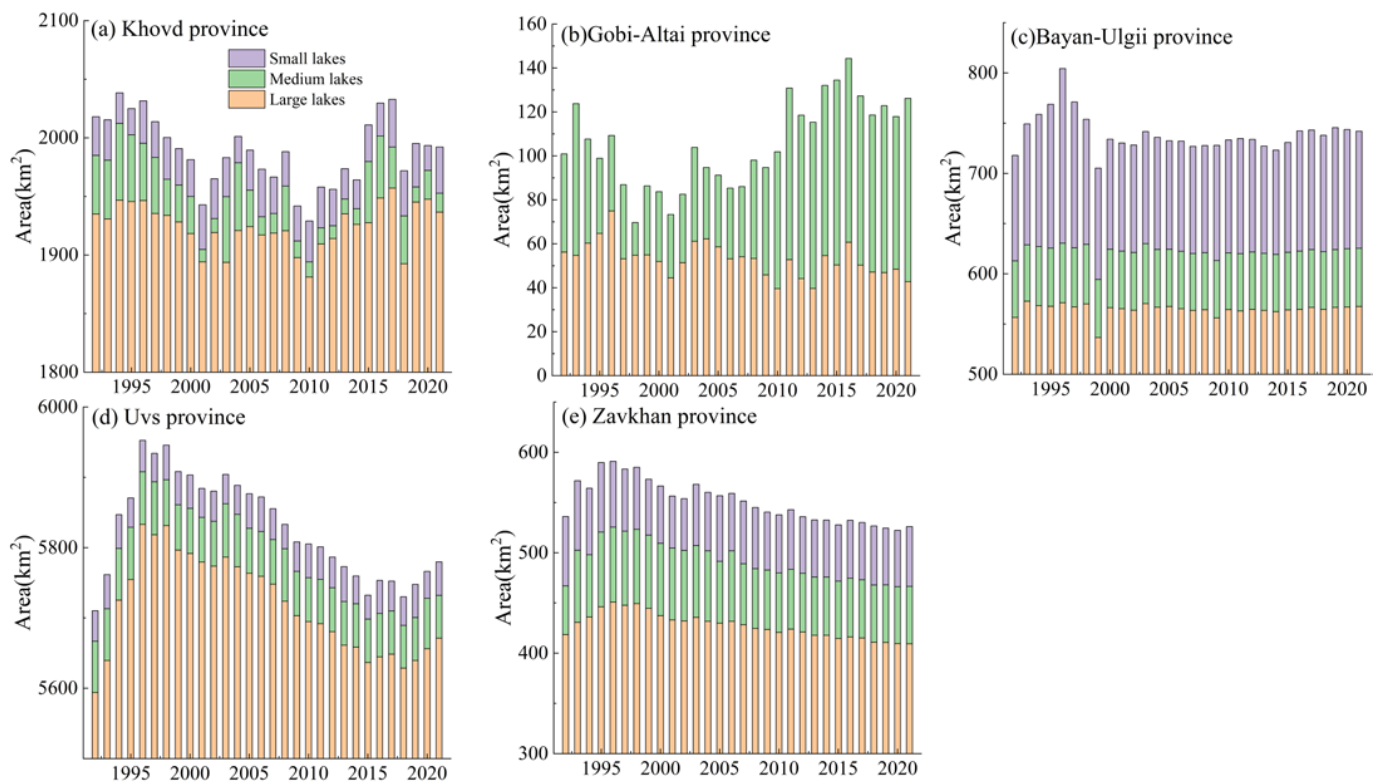


Figure 3. Interannual change of lake area and number in provinces of western Mongolia from 1992 to 2021.

4.3. Characteristic Variations in the Area of Typical Lakes

The lakes in the western region of Mongolia primarily rely on meltwater from high mountain glaciers, precipitation in mountainous areas, and river runoff for their water supply. Based on the watershed types and the sources of water supply, this study categorizes the lakes in the western region of Mongolia into alpine lakes, throughput lakes, and coccyx lakes [6] (Text S1 and Table S1).

The area of typical inland lakes in western Mongolia exhibited varying trends from 1992 to 2021 (Figure 4). Overall, high mountain lakes and tailing lakes showed an increasing trend in their respective areas, while throughput lakes exhibited a decreasing trend in their overall area. Based on the 30-year analysis of the selected typical inland lakes, it is evident that coccyx lakes have the largest water surface area, significantly exceeding the water surface area of alpine lakes and throughput lakes. Throughput lakes have the second-largest water surface area, while alpine lakes have the smallest water surface area. The water surface areas of all three lake types showed an expanding trend between 1992 and 1996. However, after 1996, the water surface areas of these lake types exhibited varying degrees of shrinkage.

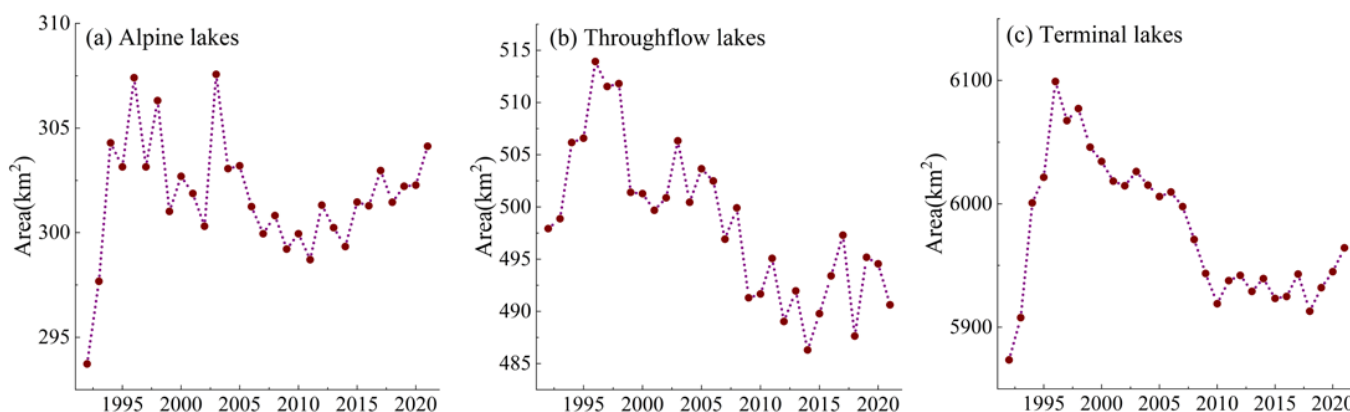


Figure 4. Interannual change in the lake area of typical lakes in western Mongolia from 1992 to 2021.

4.4. Attribution Analyses of Lake Changes in Western Mongolia

The annual precipitation in each province fluctuates greatly (Figure 5a). From 1992 to 2003, the annual precipitation in each province showed a fluctuating downward trend, with greater fluctuations after 2003. The average summer temperature and potential evapotranspiration in each province showed a fluctuating increasing trend during the study period (Figure 5b,c). Among them, from 1992 to 2002, there was a continuous upward trend, followed by greater fluctuations after 2002. In the western region of Mongolia, there is a slight variation in annual precipitation, while summer temperatures and potential evapotranspiration show a clear increasing trend. The phenomenon of climate warming and aridification is evident (Figures S3–S5). For irrigated land, there are significant differences in the trend of changes in irrigated land among provinces (Figure 5d). The change in irrigated land area in Uvs and Khovd provinces showed an inverted “U” shape. The irrigated land area in Zavkhan, Gobi-Altai, and Bayan-Ulgii provinces rapidly decreased from 1992 to 1995, with Zavkhan province experiencing the most significant decrease. After 1995, the changes in irrigated land area in the three provinces were relatively small. The livestock numbers in each province showed an increasing trend during the study period (Figure 5e). Due to the impact of severe weather [23], the livestock numbers in each province fluctuated greatly from 1992 to 2010, and relatively low values were observed in 2002 and 2010. After 2010, the livestock numbers in each province continued to increase. The western region of Mongolia has a smaller population (Figure 5f). Before 2000, the population was mainly distributed in Uvs and Zavkhan provinces. After 2000, the population mainly shifted to Bayan-Ulgii province. During the study period, Gobi-Altai, Uvs, and Zavkhan provinces experienced a population decline, while Khovd and Bayan-Ulgii provinces showed a population increase.

During the study period, the moisture changes in different depths of the soil varied (Figures 6 and S6–S9). Generally, the soil moisture in various provinces showed a fluctuating decreasing trend during the study period. Moreover, in the early stages of the study, the soil moisture primarily decreased, while in the later stages, there was a slight recovery in soil moisture. Among the different depths of the soil, the most significant decrease in soil moisture was observed in the fourth layer.

Using path analysis in structural equation modeling, we investigated the degree of influence and the pathways through which different factors affect the lake areas in various provinces (Figures 7 and S10). The results indicate that the driving factors for changes in lake areas vary across provinces. In the case of Khovd province, climate change and human activities predominantly exert an indirect influence on lake area changes, with climate change having a greater impact than human activities. For Gobi-Altai province, climate change and human activities primarily have a direct impact on lake area changes, with both factors contributing equally as driving forces. In Bayan-Ulgii province, climate change and human activities mainly have an indirect influence on lake area changes, with human activities exerting a greater influence than climate change. In Uvs province, climate change primarily affects lake areas indirectly, while human activities mainly have a

direct influence. In Zavkhan province, climate change primarily affects lake area changes indirectly, with human activities exerting an equal combination of direct and indirect effects on lake area changes.

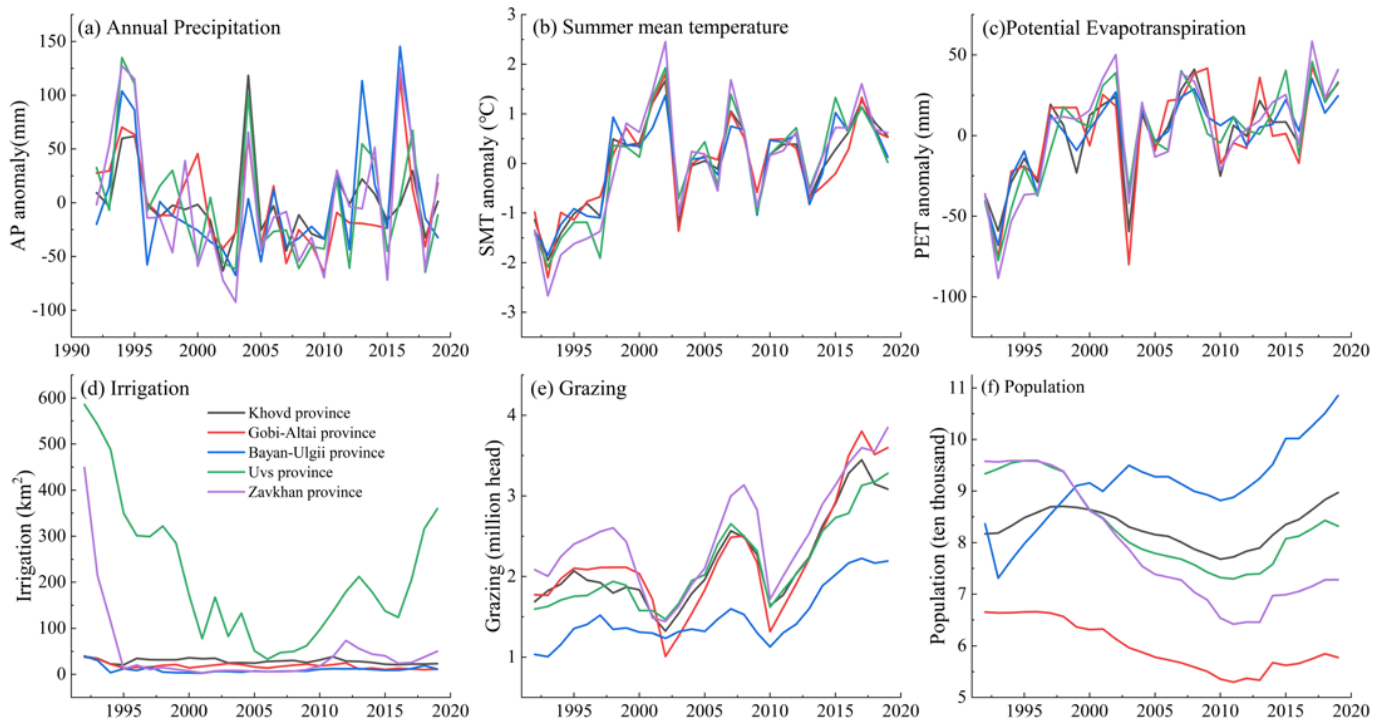


Figure 5. The changes in climate and driving factors of human activities in western Mongolia from 1992 to 2018.

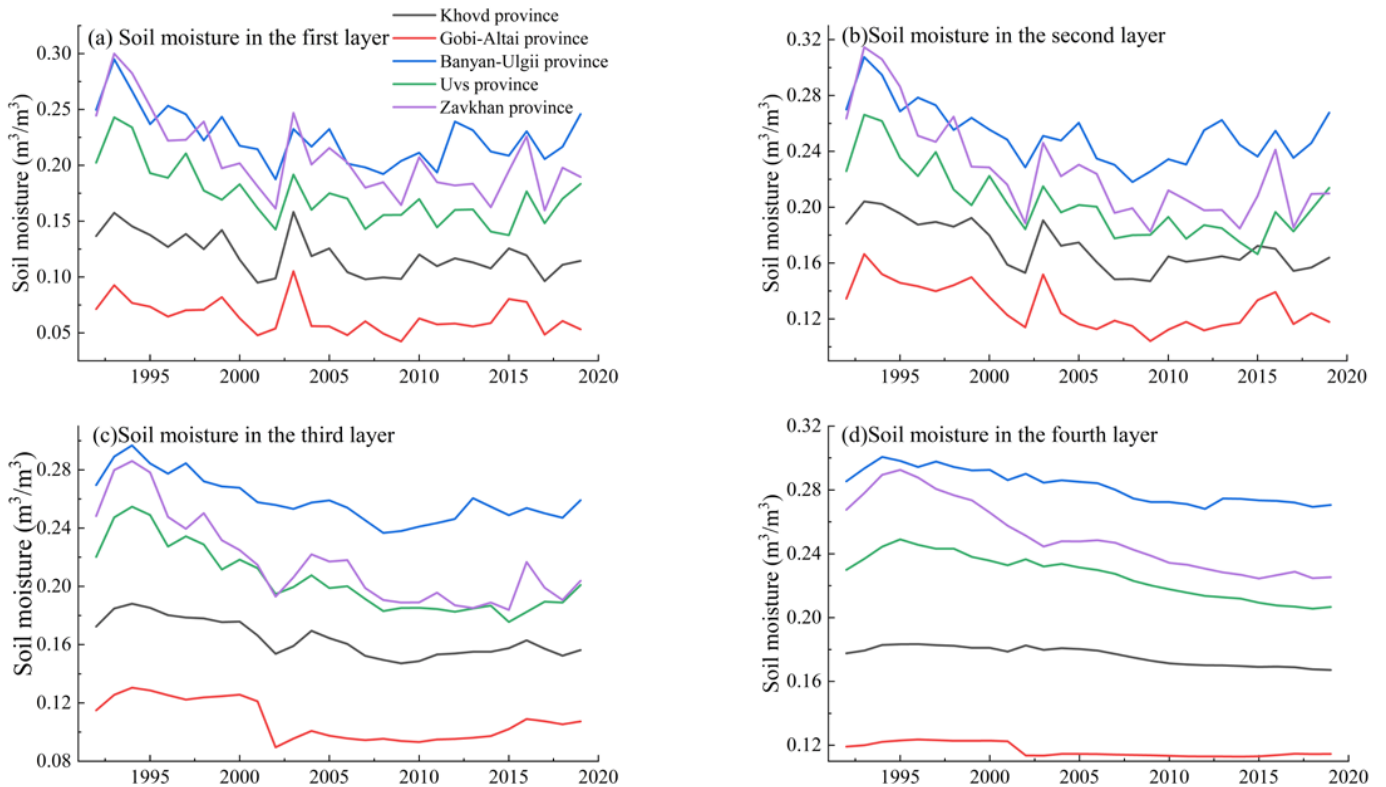


Figure 6. The changes in soil moisture in western Mongolia from 1992 to 2018.

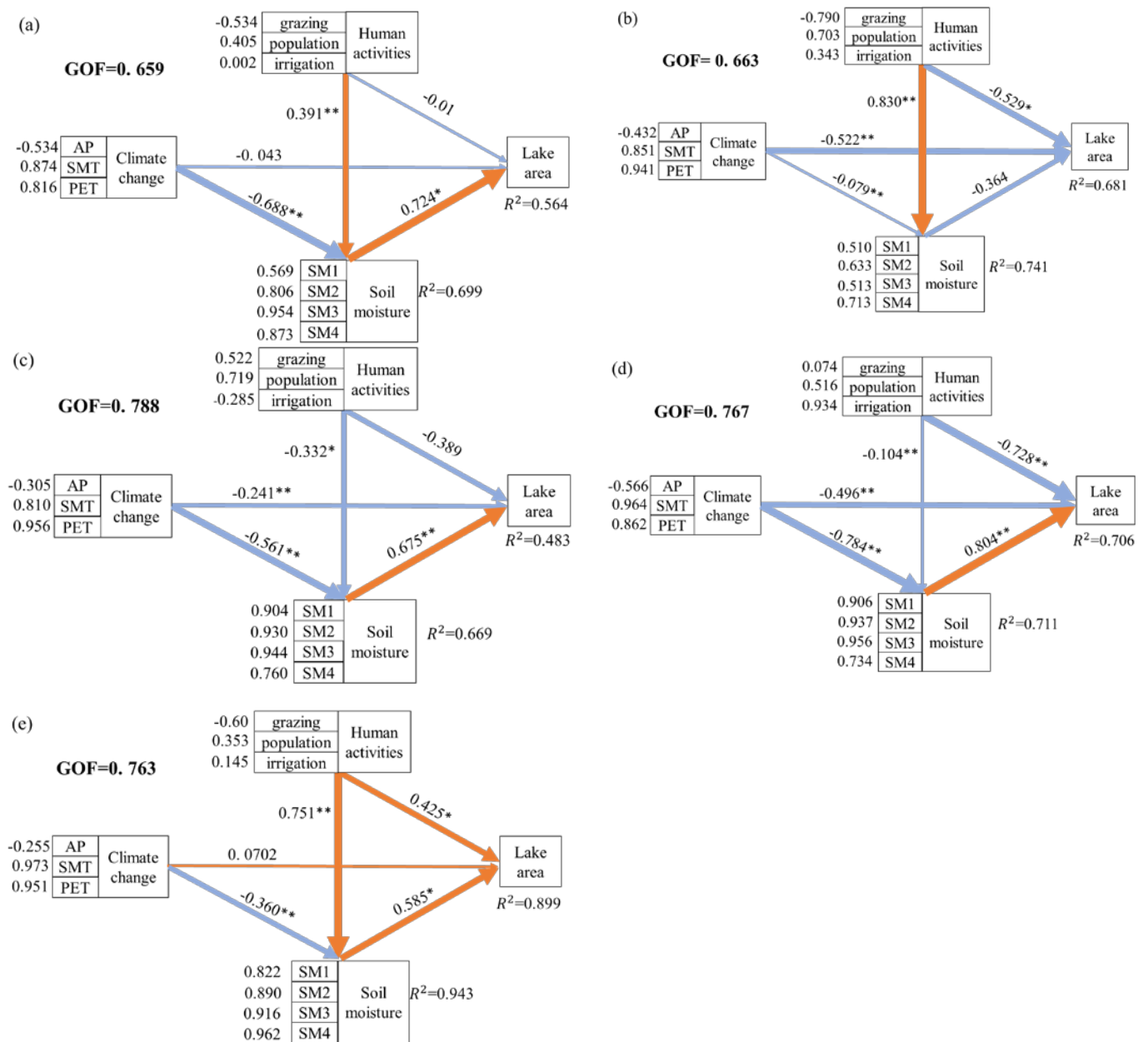


Figure 7. Structural equation modeling of climate change, human activities, and soil moisture on lake area changes in five western provinces of Mongolia (** significance level of $p < 0.01$, * significance level of $p < 0.05$). (a–e) represent the provinces of Khovd, Gobi-Altai, Bayan-Ulgii, Uvs, and Zavkhan, respectively.

Overall, climate change and human activities primarily influence changes in lake areas indirectly. Specifically, climate change and human activities lead to soil drying, which has caused a recent decline in lake areas, which is consistent with previous research. Among these factors, human activities have a direct impact on lake area changes in the Uvs province. This is mainly attributed to the extensive irrigation land distribution in the province. Agricultural irrigation extracts a significant amount of surface water and groundwater, reducing the inflow into the lakes. Climate change and human activities have an indirect impact on lake area changes in various provinces. Specifically, climate change and human activities alter soil moisture, which provides a good explanation for the changes in lake area.

We used structural equation modeling to investigate the degree of environmental factors' influence on the areas of three different types of lakes and their causal pathways (Figures 8 and S11). For alpine lakes, climate change serves as the primary driving force behind changes in lake area, with a significant direct effect of -0.719 . Specifically, the increase in summer average temperature has a strong explanatory power for the changes in the area of alpine lakes (Table 1). In the case of throughflow lakes and terminal lakes, human activities emerge as the main driving force behind changes in lake areas. However, the distinction lies in the fact that human activities primarily exert an indirect influence on the area changes of throughflow lakes, whereas they predominantly exhibit a direct influence on the area changes of terminal lakes.

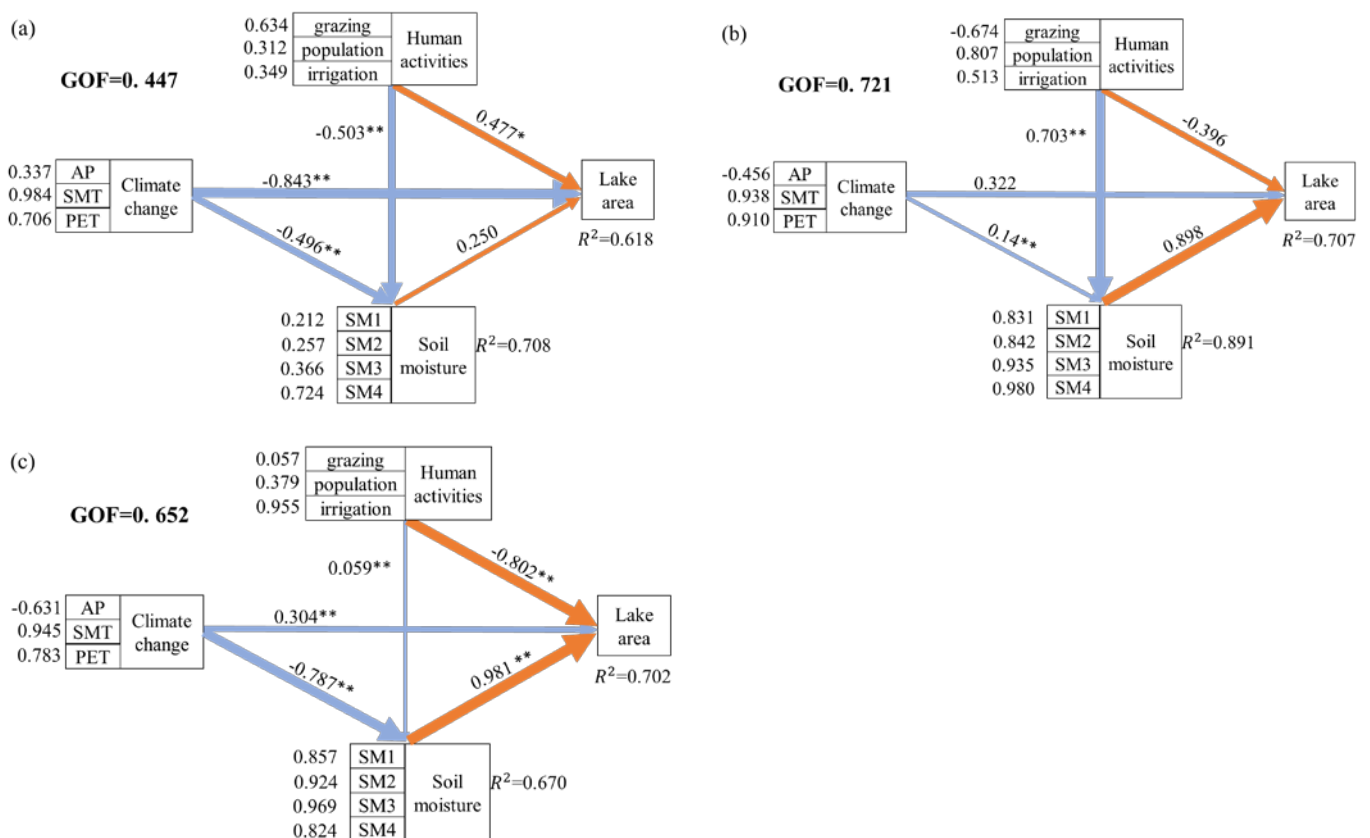


Figure 8. Structural equation modeling of climate change, human activities, and soil moisture on changes in the area of three typical inland lakes in western Mongolia (** significance level of $p < 0.01$, * significance level of $p < 0.05$). (a–c) represent alpine lakes, throughflow lakes, and terminal lakes, respectively.

Table 1. Correlation analysis between typical inland lakes and environmental factors in western Mongolia.

Types	AP	SMT	PET	Grazing	Population	Irrigation	SM1	SM2	SM3	SM4
Alpine lakes		-0.62^{**}								
Throughflow lakes				-0.48^{**}	0.625^{**}		0.49^{**}	0.54^{**}	0.65^{**}	0.82^{**}
Terminal lakes					0.474^*				0.41^{**}	0.68^{**}

** Significance level of $p < 0.01$, * significance level of $p < 0.05$; this study excluded variables that were not statistically significant ($p > 0.05$).

5. Discussion

5.1. Regional Geographical Significance of the Dynamics of Lake Area in Western Mongolia

Regional-scale lake studies play a crucial role in comprehending the response of different regions to climate change [24]. The Mongolian Plateau and the Tibetan Plateau are recognized as highly vulnerable regions to climate change [24], necessitating a multitude of studies on lake dynamics and their responses to environmental changes in typical Tibetan Plateau regions such as Qiangtang and Sanjiangyuan [25–28]. However, there remains a dearth of analyses concerning lake area changes and their driving forces in typical regions of the Mongolian Plateau. Particularly, limited research has been conducted on the mechanisms underlying lake changes in significant climatic zones like the Great Lakes Depression of Mongolia [6]. Consequently, it holds substantial practical significance to ascertain trends in lake area and quantity within the Great Lakes Depression of Mongolia, while uncovering the influencing factors and mechanisms governing such changes. Such investigations can greatly contribute to the management of water resources and the conservation of migratory birds and other biodiversity and serve as a warning mechanism for the warming and drying trends occurring in the climate of the Mongolian Plateau.

5.2. Analysis of Drivers of Lake Area Change

Lakes, as a unique type of water body, are closely related to various factors such as the atmosphere, organisms, and soil. However, current research on the factors influencing changes in lake surface area primarily focuses on the direct impacts of climate change, such as temperature, precipitation, evapotranspiration, and human activities, including grazing and irrigation agriculture [5,7]. However, it should be noted that lake changes can be influenced not only directly but also indirectly by climate change and human activities. Previous research has revealed that the sustained increase in SMT and PET on the Mongolian Plateau in recent decades has exacerbated aridification and contributed to the drying and warming of the climate [29–31]. Furthermore, enhanced land–air coupling has been linked to soil moisture deficits [14,15,32,33]. Overgrazing has led to grassland degradation, resulting in reduced soil function and water retention capacity, thereby impacting the water supply to lakes [5,7]. Additionally, agricultural irrigation has contributed to surface and groundwater depletion, exacerbating soil drying and affecting the water supply to lakes [7,34,35]. It is evident that the influence of climate change and human activities on lakes operates primarily through the mediation of soil moisture, which acts as a critical link in the hydrothermal exchange between surface water, groundwater, and atmospheric water [33,36]. Therefore, employing soil moisture as an intermediate variable to investigate the effects of climate change and human activities on lake changes can facilitate a deeper understanding of the key influencing factors and the mechanisms driving lake changes [33,36]. This approach can provide theoretical guidance for studying the driving factors and their variations in the dynamic changes of lakes in different regions and different types of lakes, as well as for the conservation of lake water source areas.

SEM is a model used to analyze the path relationships among complex variables. It has shown good performance in exploring the influence of various complex factors and has been widely applied in studying driving factors. SEM has also been used in attributing the dynamic changes in surface water area [37–41]. Previous studies have accurately identified the contributions of various environmental factors to changes in surface water area using SEM [37–41]. Path analysis has been used to categorize observed variables and explore the impact of latent variables (e.g., climate change, human activities) on surface water area that cannot be directly observed [37–41]. Furthermore, SEM has been employed to investigate the mechanisms by which environmental factors affect changes in surface water area. For example, Wang et al. (2022) [41] used the PLS-SEM model to attribute the changes in urban wetland areas and found that urbanization processes negatively influenced wetland distribution through their impact on topography, while urbanization weakened the direct positive influence of soil on the wetlands. However, the application of SEM in attributing the dynamic changes in surface water area is still limited, mainly focusing on the attribution

of individual lake area changes. There is a lack of attribution analysis for the changes in lake areas in different regions and different types of lakes within the mesoscale range.

Our quantitative analyses show that there has been a large regional variation in lake changes and their associated drivers in western Mongolia over the past decades. This variation is due to differences in lake size, topography, climate, geographic location, grazing intensity, and irrigated agricultural area between provinces. Differences in surface water resources, hydrothermal soil matches, and intensity of human activities between provinces lead to differences in the driving mechanisms of lake change. An analysis of the driving factors behind changes in the surface area of typical inland lakes in western Mongolia reveals that summer average temperature has a significant explanatory power for the variations in alpine lakes. Alpine lakes primarily consist of glacier lakes and proglacial lakes, which directly receive water supply from glacier melt. The early rise in temperature increases the water supply to the lakes through glacier melt [5,42], while in the later stages, the reduction in the storage capacity of solid water reservoirs leads to a decrease in the water supply from glacier melt to alpine lakes [5,42]. Throughflow lakes and terminal lakes are mainly located at lower elevations and within large lake basins, where the intensification of human activities serves as the main driving force behind the changes in lake surface area. This shows that it is necessary to seek the causes from the geographic and environmental characteristics of the study area, which has certain theoretical significance for improving the understanding of the process and mechanism of lake changes, and conduct an in-depth study of the environmental changes in the study area and the management of small watersheds.

5.3. Environmental Impact of Lake Desiccation

Lake shrinkage and desiccation can lead to diverse environmental impacts [43].

Waterfowl and Nature Conservation. Due to western Mongolia's geographical location between the Siberian taiga and the desert of Central Asia, geological and topographical features, and extreme climatic conditions, the distribution of vegetation cover is very unique. These natural conditions contribute to the diversity of fauna ecosystems: snow tigers and sheep in the high mountains and reptiles in the Gobi region [6,13]. Although nature reserves have been established to reduce the risks of human disturbance to wetlands [6], habitat loss and degradation still pose potential threats to the sustainability of wetland wildlife.

Sandstorm. In recent years, East Asian countries have been greatly affected by sandstorms [44,45]. The western region of Mongolia serves as the main source of sandstorms in Asia [46], and the deterioration of the ecological environment in this area has been the primary cause of the increased occurrence of sandstorms in recent years. The decrease in precipitation, rise in temperatures, overgrazing, and agricultural irrigation have resulted in the drying up or interruption of rivers and lakes, turning the dried-up lakes into new sources of sandstorms. Furthermore, the reduction in surface water area and the negative feedback between soil moisture and surface vegetation coverage have intensified regional drought and land degradation, leading to an increase in the frequency and intensity of sandstorm occurrences.

Water Quality and Water Resources. Lake shrinkage could lead to a shift from freshwater to salty water in drylands [43]. In our study area, an increase in the salinity of the lake water was observed [6]. Salt can damage the aquatic ecosystem and even fisheries and human health [43]. In addition, the shrinkage of lakes, the deterioration of lake water quality, and the rapid increase in the number of livestock in the region have exacerbated the water shortage in western Mongolia [6,13]. During drought years, a significant number of livestock die due to water scarcity, which was the case in 2010. The drying up, shrinking, and deterioration of lake water quality have led local communities to increasingly rely on groundwater for irrigating crops and feeding livestock, further accelerating the decline in the groundwater level.

In summary, our study suggests that the negative impacts of lake desiccation on ecosystem components are strongly interactive. A comprehensive assessment of climate,

water bodies, soil, wetland vegetation, and waterfowl changes in western Mongolia contributes significantly to a deeper understanding of how ecosystem services will respond to future climate change.

6. Conclusions

Lakes, as important water sources for industrial, agricultural, and human needs, have significant impacts on the environment and terrestrial ecosystems in western Mongolia. This study investigates the interannual variations of lakes in western Mongolia using land satellite remote sensing data. The research findings indicate notable phased characteristics in lake area changes, with an expanding trend observed from 1992 to 1996, followed by a decreasing trend from 1996 onwards. There are significant differences in the changes among lakes of different size categories, with large and medium-sized lakes being relatively stable, while small lakes experience a greater reduction. Provincial-scale analysis reveals a changing trend of lake area in Khovd and Gobi-Altai provinces, characterized by a decrease followed by an increase, whereas Uvs and Zavkhan provinces exhibit an increasing trend followed by a decrease. Three typical lake types, namely, alpine lakes, throughflow lakes, and terminal lakes, all show an initial increase followed by a decrease in their respective areas. The analysis of driving forces behind lake area changes indicates that climate change and human activities primarily exert indirect influences on the lake area variations in each province. Specifically, climate change and human activities lead to changes in soil moisture, which can explain the changes in lake areas effectively. For the specific lake types, climate change serves as the main driving force for alpine lakes, while human activities are the primary driving forces for throughflow lakes and terminal lakes.

Supplementary Materials: The following supporting information can be downloaded at: <https://www.mdpi.com/article/10.3390/land13030310/s1>, Text S1, Table S1 and Figures S1–S11.

Author Contributions: Resources, S.Y., Y.L. and O.D.; Data curation, S.Y., B.D. and D.B.; Writing—original draft, S.Y.; Writing—review & editing, S.Y. and H.Z.; Visualization, S.Y.; Funding acquisition, H.Z. All authors have read and agreed to the published version of the manuscript.

Funding: This research was funded by The National Key Research and Development Project of China (grant No. 2022YFE0119400), the National Science and Technology Basic Resources Survey Project of China (grant No. 2023FY100701), and the Mongolian Science and Technology Foundation (grant No. CHN-2022/274).

Data Availability Statement: The datasets used and/or analyzed during the current study are available from the corresponding author upon reasonable request.

Conflicts of Interest: The authors declare no conflict of interest.

References

1. Li, J.; Chen, X.; Bao, A. Spatial-temporal Characteristics of Lake Level Changes in Central Asia during 2003–2009. *Acta Geogr. Sin.* **2011**, *66*, 1219–1229.
2. Cao, G.; Li, T.; Lu, C.; Xu, Z. Dynamic variation and evaporation of seasonal lakes in arid areas: A case study for the Aiding Lake. *Arid Zone Res.* **2020**, *37*, 1095–1104.
3. Yang, T.; Wu, T.; Ji, X.; Qin, B.; Luan, C.; Hu, R.; He, X. Reconstruction of the depletion process of lake water resources in semi-arid areas under strong human activities-Taking Lake Daihai as an example. *J. Lake Sci.* **2022**, *34*, 2105–2121.
4. Luo, R.; Yuan, Q.Q.; Yue, L.W.; Shi, X.G. Monitoring Recent Lake Variations Under Climate Change Around the Altai Mountains Using Multimission Satellite Data. *IEEE J. Sel. Top. Appl. Earth Obs. Remote Sens.* **2021**, *14*, 1374–1388. [[CrossRef](#)]
5. Tao, S.L.; Fang, J.Y.; Zhao, X.; Zhao, S.Q.; Shen, H.H.; Hu, H.F.; Tang, Z.Y.; Wang, Z.H.; Guo, Q.H. Rapid loss of lakes on the Mongolian Plateau. *Proc. Natl. Acad. Sci. USA* **2015**, *112*, 2281–2286. [[CrossRef](#)] [[PubMed](#)]
6. Orkhonselenge, A.; Uuganzaya, M.; Davaagatan, T. *Lakes of Mongolia: Geomorphology, Geochemistry and Paleoclimatology*; Springer: Berlin/Heidelberg, Germany, 2022.
7. Zhou, Y.; Dong, J.W.; Xiao, X.M.; Liu, R.G.; Zou, Z.H.; Zhao, G.S.; Ge, Q.S. Continuous monitoring of lake dynamics on the Mongolian Plateau using all available Landsat imagery and Google Earth Engine. *Sci. Total Environ.* **2019**, *689*, 366–380. [[CrossRef](#)]
8. Sun, A.Z.; Feng, Z.D.; Ran, M.; Zhang, C.J. Pollen-recorded bioclimatic variations of the last ~22,600 years retrieved from Achit Nuur core in the western Mongolian Plateau. *Quat. Int.* **2013**, *311*, 36–43. [[CrossRef](#)]

9. Feng, Q.; Chang, Z.; Xi, H.; Su, Y.; Wen, X.; Zhu, M.; Zhang, J.; Zhang, C. Response to Global Change in the Ecologically Fragile and Desert Region of China-Mongolia Based on Carbon and Nitrogen Cycles. *Adv. Earth Sci.* **2022**, *37*, 1101–1114.
10. Fang, L.Q.; Tao, S.L.; Zhu, J.L.; Liu, Y. Impacts of climate change and irrigation on lakes in arid northwest China. *J. Arid Environ.* **2018**, *154*, 34–39. [[CrossRef](#)]
11. Huang, W.J.; Duan, W.L.; Chen, Y.N. Rapidly declining surface and terrestrial water resources in Central Asia driven by socio-economic and climatic changes. *Sci. Total Environ.* **2021**, *784*, 147193. [[CrossRef](#)]
12. Huang, W.J.; Duan, W.L.; Nover, D.; Sahu, N.; Chen, Y.N. An integrated assessment of surface water dynamics in the Irtysh River Basin during 1990–2019 and exploratory factor analyses. *J. Hydrol.* **2021**, *593*, 125905. [[CrossRef](#)]
13. Yembuu, B. *The Physical Geography of Mongolia*; Springer: Berlin/Heidelberg, Germany, 2021.
14. Lamchin, M.; Park, T.; Lee, J.Y.; Lee, W.K. Monitoring of Vegetation Dynamics in the Mongolia Using MODIS NDVIs and their Relationship to Rainfall by Natural Zone. *J. Indian Soc. Remote Sens.* **2015**, *43*, 325–337. [[CrossRef](#)]
15. Zhang, P.; Jeong, J.H.; Yoon, J.H.; Kim, H.; Wang, S.Y.S.; Linderholm, H.W.; Fang, K.Y.; Wu, X.C.; Chen, D.L. Abrupt shift to hotter and drier climate over inner East Asia beyond the tipping point. *Science* **2020**, *370*, 1095–1099. [[CrossRef](#)]
16. Han, J.; Dai, H.; Gu, Z.L. Sandstorms and desertification in Mongolia, an example of future climate events: A review. *Environ. Chem. Lett.* **2021**, *19*, 4063–4073. [[CrossRef](#)]
17. Kang, S.; Hong, S.Y. Assessing Seasonal and Inter-Annual Variations of Lake Surface Areas in Mongolia during 2000–2011 Using Minimum Composite MODIS NDVI. *PLoS ONE* **2016**, *11*, e0151395. [[CrossRef](#)]
18. Kang, S.Y.; Lee, G.; Togtokh, C.; Jang, K.C. Characterizing regional precipitation-driven lake area change in Mongolia. *J. Arid Land* **2015**, *7*, 146–158. [[CrossRef](#)]
19. Zhu, Z.; Woodcock, C.E. Automated cloud, cloud shadow, and snow detection in multitemporal Landsat data: An algorithm designed specifically for monitoring land cover change. *Remote Sens. Environ.* **2014**, *152*, 217–234. [[CrossRef](#)]
20. Wang, X.X.; Xiao, X.M.; Zou, Z.H.; Chen, B.Q.; Ma, J.; Dong, J.W.; Doughty, R.B.; Zhong, Q.Y.; Qin, Y.W.; Dai, S.Q.; et al. Tracking annual changes of coastal tidal flats in China during 1986–2016 through analyses of Landsat images with Google Earth Engine. *Remote Sens. Environ.* **2020**, *238*, 110987. [[CrossRef](#)]
21. Chen, F.; Zhang, M.M.; Tian, B.S.; Li, Z. Extraction of Glacial Lake Outlines in Tibet Plateau Using Landsat 8 Imagery and Google Earth Engine. *IEEE J. Sel. Top. Appl. Earth Obs. Remote Sens.* **2017**, *10*, 4002–4009. [[CrossRef](#)]
22. Hu, R.Y.; Wang, Y.M.; Chang, J.X.; Istanbuluoglu, E.; Guo, A.J.; Meng, X.J.; Li, Z.H.; He, B.; Zhao, Y.X. Coupling water cycle processes with water demand routes of vegetation using a cascade causal modeling approach in arid inland basins. *Sci. Total Environ.* **2022**, *840*, 156492. [[CrossRef](#)]
23. Nandintsetseg, B.; Boldgiv, B.; Chang, J.F.; Ciais, P.; Davaanyam, E.; Batbold, A.; Bat-Oyun, T.; Stenseth, N.C. Risk and vulnerability of Mongolian grasslands under climate change. *Environ. Res. Lett.* **2021**, *16*, 034035. [[CrossRef](#)]
24. Zhang, G.Q.; Yao, T.D.; Piao, S.L.; Bolch, T.; Xie, H.J.; Chen, D.L.; Gao, Y.H.; O'Reilly, C.M.; Shum, C.K.; Yang, K.; et al. Extensive and drastically different alpine lake changes on Asia's high plateaus during the past four decades. *Geophys. Res. Lett.* **2017**, *44*, 252–260. [[CrossRef](#)]
25. Dong, S.; Xue, X.; You, Q.; Peng, F. Remote sensing monitoring of the lake area changes in the Qinghai-Tibet Plateau in recent 40 years. *J. Lake Sci.* **2014**, *26*, 535–544.
26. Liu, J.; Zhou, T.; Yu, H.; Sun, J. Dynamics and Driving Forces of Lake Changes in Tibet During the Past 25 Years. *J. Yangtze River Sci. Res. Inst.* **2018**, *35*, 145–150.
27. Lu, S.J.; Si, J.H.; Hou, C.Y.; Li, Y.S.; Wang, M.M.; Yan, X.X.; Xie, M.; Sun, J.X.; Chen, B.J.; Li, S.S. Spatiotemporal distribution of nitrogen and phosphorus in alpine lakes in the Sanjiangyuan Region of the Tibetan Plateau. *Water Sci. Technol.* **2017**, *76*, 396–412. [[CrossRef](#)] [[PubMed](#)]
28. Wan, W.; Xiao, P.; Feng, X.; Li, H.; Ma, R.; Duan, H. Remote sensing analysis for changes of lakes in the southeast of Qiangtang area, Qinghai-Tibet Plateau in recent 30 years. *Sci. Limnol. Sin.* **2010**, *22*, 874–881.
29. Fukumoto, Y.; Kashima, K.; Ganzorig, U. The Holocene environmental changes in boreal fen peatland of northern Mongolia reconstructed from diatom assemblages. *Quat. Int.* **2014**, *348*, 66–81. [[CrossRef](#)]
30. Tumenjargal, S.; Fassnacht, S.R.; Venable, N.B.H.; Kingston, A.P.; Fernández-Giménez, M.E.; Batbuyan, B.; Laituri, M.J.; Kappas, M.; Adyabadam, G. Variability and change of climate extremes from indigenous herder knowledge and at meteorological stations across central Mongolia. *Front. Earth Sci.* **2020**, *14*, 286–297. [[CrossRef](#)]
31. Wang, L.; Yao, Z.J.; Jiang, L.G.; Wang, R.; Wu, S.S.; Liu, Z.F. Changes in Climate Extremes and Catastrophic Events in the Mongolian Plateau from 1951 to 2012. *J. Appl. Meteorol. Climatol.* **2016**, *55*, 1169–1182. [[CrossRef](#)]
32. Li, S.G.; Eugster, W.; Asanuma, J.; Kotani, A.; Davaa, G.; Oyunbaatar, D.; Sugita, M. Energy partitioning and its biophysical controls above a grazing steppe in central Mongolia. *Agric. For. Meteorol.* **2006**, *137*, 89–106. [[CrossRef](#)]
33. Luo, M.; Meng, F.H.; Wang, Y.Q.; Sa, C.L.; Duan, Y.C.; Bao, Y.H.; Liu, T. Quantitative detection and attribution of soil moisture heterogeneity and variability in the Mongolian Plateau. *J. Hydrol.* **2023**, *621*, 129673. [[CrossRef](#)]
34. Blanc, E.; Strzepek, K.; Schlosser, A.; Jacoby, H.; Gueneau, A.; Fant, C.; Rausch, S.; Reilly, J. Modeling US water resources under climate change. *Earths Future* **2014**, *2*, 197–224. [[CrossRef](#)]
35. Sasaki, T.; Okayasu, T.; Jamsran, U.; Takeuchi, K. Threshold changes in vegetation along a grazing gradient in Mongolian rangelands. *J. Ecol.* **2008**, *96*, 145–154. [[CrossRef](#)]

36. Luo, M.; Meng, F.H.; Sa, C.L.; Duan, Y.C.; Bao, Y.H.; Liu, T.; De Maeyer, P. Response of vegetation phenology to soil moisture dynamics in the Mongolian Plateau. *Catena* **2021**, *206*, 105505. [[CrossRef](#)]
37. Du, B.J.; Wang, Z.M.; Mao, D.H.; Li, H.Y.; Xiang, H.X. Tracking Lake and Reservoir Changes in the Nenjiang Watershed, Northeast China: Patterns, Trends, and Drivers. *Water* **2020**, *12*, 1108. [[CrossRef](#)]
38. Li, H.Y.; Mao, D.H.; Li, X.Y.; Wang, Z.M.; Wang, C.Z. Monitoring 40-Year Lake Area Changes of the Qaidam Basin, Tibetan Plateau, Using Landsat Time Series. *Remote Sens.* **2019**, *11*, 343. [[CrossRef](#)]
39. Li, X.; Zhang, F.; Shi, J.; Chan, N.W.; Cai, Y.; Cheng, C.; An, C.; Wang, W.; Liu, C. Analysis of surface water area dynamics and driving forces in the Bosten Lake basin based on GEE and SEM for the period 2000 to 2021. *Environ. Sci. Pollut. Res. Int.* **2024**, *31*, 9333–9346. [[CrossRef](#)] [[PubMed](#)]
40. Tang, L.Y.; Duan, X.F.; Kong, F.J.; Zhang, F.; Zheng, Y.F.; Li, Z.; Mei, Y.; Zhao, Y.W.; Hu, S.J. Influences of climate change on area variation of Qinghai Lake on Qinghai-Tibetan Plateau since 1980s. *Sci. Rep.* **2018**, *8*, 7331. [[CrossRef](#)]
41. Wang, C.; Ma, L.; Zhang, Y.; Chen, N.; Wang, W. Spatiotemporal dynamics of wetlands and their driving factors based on PLS-SEM: A case study in Wuhan. *Sci. Total Environ.* **2022**, *806*, 151310. [[CrossRef](#)]
42. Pan, C.G.; Kamp, U.; Munkhjargal, M.; Halvorson, S.J.; Dashtseren, A.; Walther, M. An Estimated Contribution of Glacier Runoff to Mongolia's Upper Khovd River Basin in the Altai Mountains. *Mt. Res. Dev.* **2019**, *39*, R12–R20. [[CrossRef](#)]
43. Liu, H.Y.; Yin, Y.; Piao, S.L.; Zhao, F.J.; Engels, M.; Ciais, P. Disappearing Lakes in Semiarid Northern China: Drivers and Environmental Impact. *Environ. Sci. Technol.* **2013**, *47*, 12107–12114. [[CrossRef](#)] [[PubMed](#)]
44. Chen, F.H.; Chen, S.Q.; Zhang, X.; Chen, J.H.; Wang, X.; Gowan, E.J.; Qiang, M.R.; Dong, G.H.; Wang, Z.L.; Li, Y.C.; et al. Asian dust-storm activity dominated by Chinese dynasty changes since 2000 BP. *Nat. Commun.* **2020**, *11*, 992. [[CrossRef](#)] [[PubMed](#)]
45. Chen, Q.C.; Wang, M.M.; Sun, H.Y.; Wang, X.; Wang, Y.Q.; Li, Y.G.; Zhang, L.X.; Mu, Z. Enhanced health risks from exposure to environmentally persistent free radicals and the oxidative stress of PM_{2.5} from Asian dust storms in Erenhot, Zhangbei and Jinan, China. *Environ. Int.* **2018**, *121*, 260–268. [[CrossRef](#)] [[PubMed](#)]
46. Zhang, Y.; Mao, C.; Zhang, J.; Huang, X.; Otgonbayar, D. Aeolian activities in the NW Mongolia during the Holocene recorded by grain-sizesensitive particles in the sediments of Lake Tolbo. *J. Lake Sci.* **2023**, *35*, 368–380.

Disclaimer/Publisher's Note: The statements, opinions and data contained in all publications are solely those of the individual author(s) and contributor(s) and not of MDPI and/or the editor(s). MDPI and/or the editor(s) disclaim responsibility for any injury to people or property resulting from any ideas, methods, instructions or products referred to in the content.